A Quadratically-Constrained Convex Approximation for the AC Optimal Power Flow

Gonzalo E. Constante-Flores, *Member, IEEE,* Can Li

***Abstract*—We introduce a quadratically-constrained approximation (QCAC) of the AC optimal power flow (AC-OPF) problem. Unlike existing approximations like the DC-OPF, our model does not rely on typical assumptions such as high reactance-to-resistance ratio, near-nominal voltage magnitudes, or small angle differences, and preserves the structural sparsity of the original AC power flow equations, making it suitable for decentralized power systems optimization problems. To achieve this, we reformulate the AC-OPF problem as a quadratically constrained quadratic program. The nonconvex terms are expressed as differences of convex functions, which are then convexified around a base point derived from a warm start of the nodal voltages. If this linearization results in a non-empty constraint set, the convexified constraints form an inner convex approximation. Our experimental results, based on Power Grid Library instances of up to 30,000 buses, demonstrate the effectiveness of the QCAC approximation with respect to other well-documented conic relaxations. We further showcase its potential advantages over the well-documented second-order conic relaxation of the power flow equations in two proof-of-concept case studies: optimal reactive power dispatch in transmission networks and PV hosting capacity in distribution grids.**

***Index Terms*—AC optimal power flow, Convex approximation, Difference-of-convex programming, PV hosting capacity, Optimal reactive power dispatch, Taylor series.**

NOMENCLATURE

Sets:

$\mathcal{G}$	Generating units.
$\mathcal{N}$	Nodes in the electric network.
$\mathcal{E}$	Set of branches.
$\mathcal{E}_i$	Set of branches connected to node i.

Constants:

$\overline{B}_i/\underline{B}_i$	Maximum/Minimum shunt susceptance at node i.
B_{ij}^{sh}	Shunt susceptance of transmission line between nodes i and j.
$G_i^{\mathrm{sh}}/B_i^{\mathrm{sh}}$	Shunt conductance/susceptance at node i.
G_{ij}/B_{ij}	Series conductance/susceptance of the branch between nodes i and j.
$\overline{N}_i^{\mathrm{sh}}$	Maximum step of shunt compensation at node i.
$P_i^{\mathrm{d}}/Q_i^{\mathrm{d}}$	Active/Reactive power demand at node i.
$\overline{P}_k/\underline{P}_k$	Maximum/Minimum active power output of unit k.
$\overline{Q}_k/\underline{Q}_k$	Maximum/Minimum reactive power output of unit k.
$\overline{S}_{ij}$	Maximum apparent power flow through the branch between nodes i and j.
T_{ij}	Tap ratio of the transformer between nodes i and j.
$\overline{V}_i/\underline{V}_i$	Maximum/Minimum voltage magnitude at node i.

Variables:

b_i^{sh}	Shunt susceptance at node i.
c_{ii}	Squared voltage magnitude at node i.
c_{ij}, s_{ij}	Lifted voltage variables.
n_i^{sh}	Integer step of shunt compensation at node i.
$p_k^{\mathrm{g}}/q_k^{\mathrm{g}}$	Active/Reactive power produced by unit k.
p_{ij}/q_{ij}	Active/Reactive power flow from node i to node j.
p_{ji}/q_{ji}	Active/Reactive power flow from node j to node i.
q_i^{sh}	Reactive power produced by shunt compensation at node i.
$v_i^{\mathrm{re}}/v_i^{\mathrm{im}}$	Real/Imaginary part of voltage at node i.

Functions:

$C_k(\cdot)$	Cost function of unit k.

G. E. Constante-Flores and C. Li are with the Davidson School of Chemical Engineering, Purdue University, West Lafayette, IN 47907, USA.

I. INTRODUCTION

POWER systems are undergoing important changes due to the pervasive electrification of transportation and industry sectors and the increasing share of renewable energy resources. System operators must rely on reliably solving the AC Optimal Power Flow (AC-OPF) problem to ensure economically efficient and secure planning and operation decisions. The main challenge of reliably solving the AC-OPF comes from the nonconvexity of the power flow equations, which describe the steady-state governing physical laws of the transmission network [1].

In recent years, significant efforts have been devoted to developing more tractable linear and convex relaxations of the power flow equations, which can be reliably solved using state-of-the-art optimization solvers. In particular, these efforts include the semi-definite programming [2], second-order cone [3], and the quadratic convex [4] relaxations. The key features of convex relaxations are their ability to provide infeasibility certificates, lower bounds on the optimal objective values, and globally optimal decisions when tight. The main drawbacks of using relaxations include the overestimation of power losses [5], relaxations of Ohm's law [6], and their inability to leverage AC base solutions, also known as warm starts, from previously solved instances.

Another line of research is focused on developing tractable model-based approximations of the power flow equations [7]. One of the main advantages of such approximations is that the can (i) use solutions of previous operating conditions [8], (ii) leverage variable estimates from the solution of the state estimator for real-time applications, (iii) employ engineering assumptions [9], *e.g.,* reactance-to-resistance ratio, flat voltage magnitudes, or angle differences, and/or (iv) reduce the approximation error based on iterative procedures [10]. More recently, these approximations can be applied to exploit the accuracy and inference speed of learning-based approaches,

using the solution of historical (or synthetically generated) instances to predict base points [11].

Various approximations of the power flow equations rely on a truncated first-order Taylor series expansion of the nonconvex terms arising from the product of complex voltages. The difference between linear approximations using Taylor series lies in the selection of the independent variables, voltage magnitudes v and phase angles θ, to perform the truncated expansion. Zhang *et al.* [12] derives a linear power flow model using the v and θ as independent variables. Yang *et al.* [13] refines such linear model by using v^2 and θ, and consider the impact of v on network losses in [14]. Fatemi *et al.* [15] use v^2 and $v^2\theta$ as independent variables and introduce an adjustment factor to minimize estimation errors. Li *et al.* in [16] propose a logarithmic transform of voltage magnitudes, preserving the impact of voltage magnitudes and network losses on the active and reactive load flows. Yang *et al.* [17] derive a general formulation, where the power injections are expressed as functions of the independent variables, for selecting independent variables that render a linear power flow with reduced errors. Fan *et al.* [18] formulate a model to find a linear model with reduced linearization error by selecting the optimal independent variables for each bus. Long *et al.* in [19] propose a clustering-based approach to select the best linear power flow model depending on the similarity of the linearization error features of different operating conditions.

The authors in [20] and [10] propose the IV-Flow model, a linear approximation of the power flow equations by formulating the active and reactive power flow equations in rectangular coordinates in terms of voltages and currents and linearizing them using a first-order Taylor series expansion. Such approximation, along with the linearization of other constraints of the AC-OPF problem, is iteratively solved until a convergence criterion is satisfied. Mhanna and Mancarella [21] propose a sequential linear programming approach based on the construction of supporting hyperplanes and halfspaces and the exclusive solution of linear programming problems. Coffrin and Van Hentenryck [8] propose the LPAC model, which relies on a convex approximation of the cosine terms in the power flow equations and a Taylor approximation of the remaining nonlinear terms. Bolognani and Dörfler [22] propose an implicit linearization of the power flow manifold with a bound on the worst-case error.

On the other hand, first-order Taylor series expansions can also be applied to derive convex approximations, where all the convexities are preserved in the model while the nonconvexities are linearized. Jabr in [3] proposes a second-order conic (SOC) approximation based on his SOC relaxation, where the quadratic equality constraints are relaxed into a convex inequality and the nonconvex (arctangent) constraints are linearized. Coffrin *et al.* in [23] derive a quadratic programming approximation based on a second-order Taylor series expansion of the sine and cosine functions, assuming a near-nominal voltage magnitude approximation and a small angle difference, and on the relaxation of the quadratic equality constraints into inequalities. Baradar and Hesamzadeh in [24] propose a conic approximation of the OPF problem, assuming near nominal voltage magnitudes and small angle differences, expressed in terms of voltage magnitudes, power injections, and power losses. Šepetanc and Pandžić in [25] propose a second-order Taylor approximation of the AC power flows in polar coordinates by distributing power losses to both branch ends, and they assess its accuracy in a unit commitment problem.

Merkli *et al.* [26] formulate the AC power flow problem as a nonconvex quadratically constrained linear problem aiming at minimizing the deviation of power generation from given setpoints. The problem is reformulated as a difference-of-convex functions programming problem and solved using a difference-of-convex functions algorithm. The main limitations of such work are threefold: (i) the computational complexity of splitting the indefinite matrices in the nonconvex quadratic constraints, which relies on their full eigendecomposition (which takes $\mathcal{O}(n^3)$ time), (ii) the matrices to be split depend on the network topology, which makes such decomposition impractical in scenarios where the topology varies as it requires a new decomposition each time the topology is altered, and (iii) the convexified constraints do not preserve the sparsity of the original ones and are generally dense, which is computationally challenging for optimization solvers in terms of internal operations and memory usage.

To bridge this gap, this paper proposes a quadratically-constrained convex approximation of the AC-OPF problem (QCAC) that does not rely on typical engineering assumptions such as high reactance-to-resistance ratio, near-nominal voltage magnitudes, or small angle differences while preserving the structural sparsity of the original nonconvex constraints. The proposed QCAC approximation is derived by lifting the AC-OPF in rectangular coordinates, which allows a reformulating as a difference-of-convex functions programming problem. The reformulated problem problem is then convexified around a given set of nodal voltages. The proposed QCAC approximation shows two important features: (i) it retains all the convex information of the nonconvex voltage relationships and solely linearize their concave term, unlike other linear approximations, and (ii) it does not make any additional assumptions in terms of angle differences, reactance-to-resistance ratio, or voltage magnitudes. The accuracy and computational performance of the proposed approximation is numerically tested using realistic test systems up to 30,000 buses and two proof-of-concept case studies in transmission and distribution grids.

The remainder of this paper is organized as follows: Section II presents the formulation of the AC-OPF problem in rectangular coordinates and derives the proposed QCAC approximation. Section III illustrates the numerical performance of the proposed approximation with respect to the SOC and SDP outer approximations. Section IV demonstrates two case studies of potential applications of the proposed model. Section VI concludes the paper.

II. Proposed Quadratically-Constrained Convex Approximation of the AC-OPF Problem

Next, we present the general formulation of the AC-OPF problem in lifted rectangular coordinates and derive the proposed quadratically-constrained approximation.

A. Problem Formulation

The AC-OPF problem in lifted rectangular coordinates can be formulated as follows:

$$\min_{\Xi} \quad \sum_{k\in\mathcal{G}} C_k(p_k^{\mathrm{g}}) \tag{1a}$$

subject to

$$\sum_{k\in\mathcal{G}_i} p_k^{\mathrm{g}} - P_i^{\mathrm{d}} - G_i^{\mathrm{sh}} c_{ii} = \sum_{(i,j)\in\mathcal{E}_i} p_{ij} + \sum_{(j,i)\in\mathcal{E}_i} p_{ji},\ \forall i\in\mathcal{N}, \tag{1b}$$

$$\sum_{k\in\mathcal{G}_i} q_k^{\mathrm{g}} - Q_i^{\mathrm{d}} + B_i^{\mathrm{sh}} c_{ii} = \sum_{(i,j)\in\mathcal{E}_i} q_{ij} + \sum_{(j,i)\in\mathcal{E}_i} q_{ji},\ \forall i\in\mathcal{N}, \tag{1c}$$

$$p_{ij} = \frac{G_{ij}}{T_{ij}^2} c_{ii} - \frac{G_{ij}}{T_{ij}} c_{ij} + \frac{B_{ij}}{T_{ij}} s_{ij},\ \forall (i,j)\in\mathcal{E}, \tag{1d}$$

$$p_{ji} = G_{ij} c_{jj} - \frac{G_{ij}}{T_{ij}} c_{ij} - \frac{B_{ij}}{T_{ij}} s_{ij},\ \forall (i,j)\in\mathcal{E}, \tag{1e}$$

$$q_{ij} = -\frac{B_{ij}+B_{ij}^{\mathrm{sh}}}{T_{ij}^2} c_{ii} + \frac{G_{ij}}{T_{ij}} s_{ij} + \frac{B_{ij}}{T_{ij}} c_{ij},\ \forall (i,j)\in\mathcal{E}, \tag{1f}$$

$$q_{ji} = -\left(B_{ij}+B_{ij}^{\mathrm{sh}}\right) c_{jj} - \frac{G_{ij}}{T_{ij}} s_{ij} + \frac{B_{ij}}{T_{ij}} c_{ij},\ \forall (i,j)\in\mathcal{E}, \tag{1g}$$

$$(p_{ij})^2 + (q_{ij})^2 \le \overline{S}_{ij}^2,\ \forall (i,j),(j,i)\in\mathcal{E}, \tag{1h}$$

$$\underline{V}_i^2 \le c_{ii} \le \overline{V}_i^2,\ \forall i\in\mathcal{N}, \tag{1i}$$

$$\underline{P}_k \le p_k^{\mathrm{g}} \le \overline{P}_k,\ \forall k\in\mathcal{G}, \tag{1j}$$

$$\underline{Q}_k \le q_k^{\mathrm{g}} \le \overline{Q}_k,\ \forall k\in\mathcal{G}, \tag{1k}$$

$$c_{ii} = \left(v_i^{\mathrm{re}}\right)^2 + \left(v_i^{\mathrm{im}}\right)^2,\ \forall i\in\mathcal{N}, \tag{1l}$$

$$c_{ij} = v_i^{\mathrm{re}} v_j^{\mathrm{re}} + v_i^{\mathrm{im}} v_j^{\mathrm{im}},\ \forall (i,j)\in\mathcal{E}, \tag{1m}$$

$$s_{ij} = v_i^{\mathrm{re}} v_j^{\mathrm{im}} - v_j^{\mathrm{re}} v_i^{\mathrm{im}},\ \forall (i,j)\in\mathcal{E}, \tag{1n}$$

where the optimization variables are elements of the set

$$\Xi = \{p_k^{\mathrm{g}}, q_k^{\mathrm{g}}, p_{ij}^{\mathrm{fr}}, q_{ij}^{\mathrm{fr}}, p_{ij}^{\mathrm{to}}, q_{ij}^{\mathrm{to}}, c_{ii}, c_{ij}, s_{ij}, v_i^{\mathrm{re}}, v_i^{\mathrm{im}}\}.$$

The objective function (1a) aims at minimizing the total production cost. Constraints (1b) and (1c) enforce the active and reactive power balance, respectively. Constraints (1d)-(1g) define the active and reactive power flows throughout the power grid. Constraints (1h) enforce the thermal capacity of the branches. Constraints (1i) bound the squared voltage magnitudes. Constraints (1j)-(1k) bound the generating units' active and reactive power output, respectively. Constraints (1l)-(1n) are the nonconvex relationships between the voltage variables, v_i^{re} and v_i^{im}, and the lifted voltage variables, c_{ii}, c_{ij} and s_{ij}. Note that the nonconvexities of the AC-OPF are enclosed solely in the nonconvex quadratic constraints (1l)-(1n).

B. The QCAC Approximation of the AC Optimal Power Flow

The formulation of the AC-OPF problem (1) is amenable to be formulated as a difference-of-convex-functions programming problem, which is then convexified using a first-order Taylor series approximation of the concave terms. This subsection details the procedure to derive the proposed QCAC approximation.

The nonconvexities of Problem (1) are in the form of bivariate products, $z = xy$ with continuous variables x and y, which satisfy the following equality

$$xy = \frac{1}{4}(x+y)^2 - \frac{1}{4}(x-y)^2, \tag{2}$$

which corresponds to the difference of two convex functions. This equality makes it suitable for the AC-OPF problem to be formulated as a difference-of-convex functions optimization problem. Thus, the nonconvex equality constraints (1l)-(1n) can be expressed as inequality constraints and we can reformulate each bilinear/quadratic term as a difference of convex functions using the equality (2), which renders the following problem:

$$\min_{\Xi} \quad (1a)$$

subject to

$$(1b) - (1k),$$

$$c_{ii} \ge (v_i^{\mathrm{re}})^2 + (v_i^{\mathrm{im}})^2,\ \forall i\in\mathcal{N}, \tag{3a}$$

$$c_{ii} \le (v_i^{\mathrm{re}})^2 + \left(v_i^{\mathrm{im}}\right)^2,\ i\in\mathcal{N}, \tag{3b}$$

$$(v_i^{\mathrm{re}}+v_j^{\mathrm{re}})^2 + (v_i^{\mathrm{im}}+v_j^{\mathrm{im}})^2 - 4c_{ij} \le (v_i^{\mathrm{re}}-v_j^{\mathrm{re}})^2 + (v_i^{\mathrm{im}}-v_j^{\mathrm{im}})^2, \quad \forall (i,j)\in\mathcal{E}, \tag{3c}$$

$$(v_i^{\mathrm{re}}-v_j^{\mathrm{re}})^2 + (v_i^{\mathrm{im}}-v_j^{\mathrm{im}})^2 + 4c_{ij} \le (v_i^{\mathrm{re}}+v_j^{\mathrm{re}})^2 + (v_i^{\mathrm{im}}+v_j^{\mathrm{im}})^2, \quad \forall (i,j)\in\mathcal{E}, \tag{3d}$$

$$(v_i^{\mathrm{re}}-v_j^{\mathrm{im}})^2 + (v_j^{\mathrm{re}}+v_i^{\mathrm{im}})^2 + 4s_{ij} \le (v_i^{\mathrm{re}}+v_j^{\mathrm{im}})^2 + (v_j^{\mathrm{re}}-v_i^{\mathrm{im}})^2, \quad \forall (i,j)\in\mathcal{E}, \tag{3e}$$

$$(v_i^{\mathrm{re}}+v_j^{\mathrm{im}})^2 + (v_j^{\mathrm{re}}-v_i^{\mathrm{im}})^2 - 4s_{ij} \le (v_i^{\mathrm{re}}-v_j^{\mathrm{im}})^2 + (v_j^{\mathrm{re}}+v_i^{\mathrm{im}})^2, \quad \forall (i,j)\in\mathcal{E}. \tag{3f}$$

Note that Problem (3) is an exact reformulation of the AC-OPF problem, which is still a nonconvex problem due to the convex terms in the right-hand side of inequalities (3b)-(3f). The above reformulation admits various (piecewise-)linearizations since the nonconvexities in the right-hand side of the inequalities can be expressed as separable functions. The drawback of piecewise linearizations is the need to enforce SOS2 constraints, which renders a mixed-integer second-order conic problem. In this paper, to retain the continuous nature of the AC-OPF problem, we propose to linearize such terms using a first-order Taylor series approximation around given nodal voltages, V_i^{re} and V_i^{im}, rendering the following QCAC approximation:

$$\min_{\Xi} \quad \sum_{k\in\mathcal{G}} C_k(p_k^{\mathrm{g}}) + \rho\left[\sum_{i\in\mathcal{N}} \xi_i^{\mathrm{c}} + \sum_{(i,j)\in\mathcal{E}} \left(\xi_{ij}^{\mathrm{c}} + \xi_{ij}^{\mathrm{s}}\right)\right] \tag{4a}$$

subject to

$$(1b) - (1k),$$

$$c_{ii} \ge (v_i^{\mathrm{re}})^2 + (v_i^{\mathrm{im}})^2,\ \forall i\in\mathcal{N}, \tag{4b}$$

$$c_{ii} \le 2\left(V_i^{\mathrm{re}} v_i^{\mathrm{re}} + V_i^{\mathrm{im}} v_i^{\mathrm{im}}\right) - \left(\left(V_i^{\mathrm{re}}\right)^2 + \left(V_i^{\mathrm{im}}\right)^2\right) + \xi_i^{\mathrm{c}},\ \forall i\in\mathcal{N}, \tag{4c}$$

$$
\begin{aligned}
&(v_i^{\mathrm{re}} + v_j^{\mathrm{re}})^2 + (v_i^{\mathrm{im}} + v_j^{\mathrm{im}})^2 - 4c_{ij} \leq \xi_{ij}^{\mathrm{c}} + \\
&\quad 2(v_i^{\mathrm{re}} - v_j^{\mathrm{re}})(V_i^{\mathrm{re}} - V_j^{\mathrm{re}}) + \\
&\quad 2(v_i^{\mathrm{im}} - v_j^{\mathrm{im}})(V_i^{\mathrm{im}} - V_j^{\mathrm{im}}) - \\
&\quad \left[(V_i^{\mathrm{re}} - V_j^{\mathrm{re}})^2 + (V_i^{\mathrm{im}} - V_j^{\mathrm{im}})^2\right], \ \forall (i,j) \in \mathcal{E}, \qquad (4\mathrm{d}) \\
&(v_i^{\mathrm{re}} - v_j^{\mathrm{re}})^2 + (v_i^{\mathrm{im}} - v_j^{\mathrm{im}})^2 + 4c_{ij} \leq \xi_{ij}^{\mathrm{c}} + \\
&\quad 2(v_i^{\mathrm{re}} + v_j^{\mathrm{re}})(V_i^{\mathrm{re}} + V_j^{\mathrm{re}}) + \\
&\quad 2(v_i^{\mathrm{im}} + v_j^{\mathrm{im}})(V_i^{\mathrm{im}} + V_j^{\mathrm{im}}) - \\
&\quad \left[(V_i^{\mathrm{re}} + V_j^{\mathrm{re}})^2 + (V_i^{\mathrm{im}} + V_j^{\mathrm{im}})^2\right], \ \forall (i,j) \in \mathcal{E}, \qquad (4\mathrm{e}) \\
&(v_i^{\mathrm{re}} - v_j^{\mathrm{im}})^2 + (v_j^{\mathrm{re}} + v_i^{\mathrm{im}})^2 + 4s_{ij} \leq \xi_{ij}^{\mathrm{s}} + \\
&\quad 2(v_i^{\mathrm{re}} + v_j^{\mathrm{im}})(V_i^{\mathrm{re}} + V_j^{\mathrm{im}}) + \\
&\quad 2(v_j^{\mathrm{re}} - v_i^{\mathrm{im}})(V_j^{\mathrm{re}} - V_i^{\mathrm{im}}) - \\
&\quad \left[(V_i^{\mathrm{re}} + V_j^{\mathrm{im}})^2 + (V_j^{\mathrm{re}} - V_i^{\mathrm{im}})^2\right], \ \forall (i,j) \in \mathcal{E}, \qquad (4\mathrm{f}) \\
&(v_i^{\mathrm{re}} + v_j^{\mathrm{im}})^2 + (v_j^{\mathrm{re}} - v_i^{\mathrm{im}})^2 - 4s_{ij} \leq \xi_{ij}^{\mathrm{s}} + \\
&\quad 2(v_i^{\mathrm{re}} - v_j^{\mathrm{im}})(V_i^{\mathrm{re}} - V_j^{\mathrm{im}}) + \\
&\quad 2(v_j^{\mathrm{re}} + v_i^{\mathrm{im}})(V_j^{\mathrm{re}} + V_i^{\mathrm{im}}) - \\
&\quad \left[(V_i^{\mathrm{re}} - V_j^{\mathrm{im}})^2 + (V_j^{\mathrm{re}} + V_i^{\mathrm{im}})^2\right], \ \forall (i,j) \in \mathcal{E}, \qquad (4\mathrm{g}) \\
&\xi_i^{\mathrm{c}} \geq 0, \ \forall i \in \mathcal{N}, \qquad (4\mathrm{h}) \\
&\xi_{ij}^{\mathrm{c}} \geq 0, \ \forall (i,j) \in \mathcal{E}, \qquad (4\mathrm{i}) \\
&\xi_{ij}^{\mathrm{s}} \geq 0, \ \forall (i,j) \in \mathcal{E}, \qquad (4\mathrm{j})
\end{aligned}
$$

where ξ_i^{c}, ξ_{ij}^{c}, and ξ_{ij}^{s} are nonnegative slack variables and ρ denotes a penalty coefficient.

If the slack variables are set to zero and the convexification points, V_i^{re} and V_i^{im}, render a nonempty constraint set, Problem (4) corresponds to an inner approximation of the AC-OPF problem. However, when the base points V_i^{re} and V_i^{im} render an empty constraint set, e.g., they are infeasible to the original constraint set, we can add the aforementioned nonnegative slack variables to relax such constraints. Notice that by adding the slack variables and penalizing them in the objective function, the problem is neither an inner nor an outer approximation of the original problem. Hence, it cannot provide valid upper or lower bounds on the optimal value of the objective function, respectively.

C. Advantages of the QCAC approximation

The main advantages of the proposed approximation over other linearization-based approaches, e.g., the sequential quadratic programming algorithm, and models based on linearization of the nonconvexities via first-order Taylor series expansion, are the following:

1) The convexified constraints retain more information with respect to other linear approximations since they preserve all the information of the convex component of each nonconvex term and only linearize its concave part [27]. Conversely, in the linearization-based approaches, the second-order information is the objective constraints and/or constraints is lost. Figure 1 illustrates in a simple difference-of-convex (nonconvex) constraint, $y \geq x^2 - |x|$, the approximate convex set obtained using the proposed convex approximation and the one obtained a standard first-order Taylor series linearization.

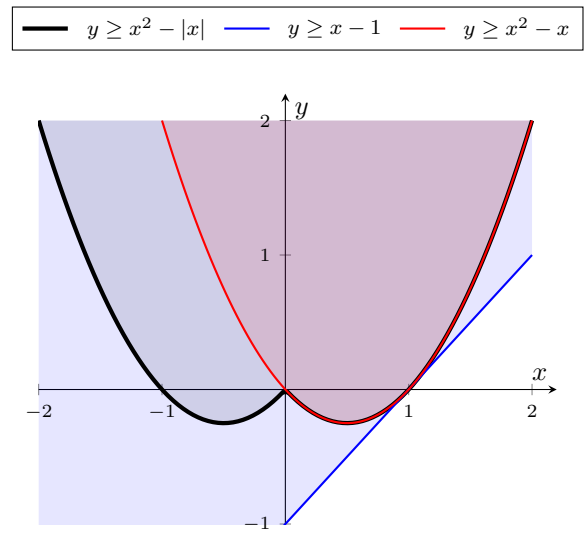

Fig. 1. Illustration of difference-of-convex function (nonconvex) constraint (black), and first-order Taylor series linearization (blue) and proposed convex approximation (red) around $x = 1$. Note that the proposed convexification is tight for $x \geq 0$ whereas the first-order Taylor series linearization is tight only at the linearization point $x = 1$.

2) The proposed approximation preserves the structure and sparsity of the original AC power flow equations. Each convexified constraint, (4b)-(4g), depends on variables pertaining to the corresponding bus or branch. This fact enables the application of the QCAC approximation in settings where such feature is imperative, such as decentralized operation of power systems.
3) The QCAC approximation can be used along learning-based techniques that can leverage historical (or synthetically generated) instances to learn the mapping between nodal demands and nodal voltages, which correspond to our convexification points [11]. Notice that since the QCAC approximation is convex, it can be embedded within the training pipeline of a learning model as a differentiable layer, enabling the use of packages like DiffOpt.jl [28] and CVXPYLayers [29] to automate the computation of the gradients.

III. Numerical experiments

In this section, we provide numerical experiments to evaluate the performance of the proposed QCAC approximation in terms of feasibility, optimality gap, and runtime. The data of the studied instances can be retrieved from the PGLIB-OPF library [30]. The numerical experiments have been implemented on a Macbook Pro laptop with an Apple M2 Pro processor and 32 GB of RAM under JuMP 1.10 with Mosek 10.1.2 as the optimization solver.

A. Experimental setup

The results of the proposed QCAC approximation are compared with the ones of a second-order conic [3] and semidefinite relaxation [2] for selected systems up to 1354 buses. For larger systems of 6,495, 13,659, and 30,000 buses, we study the performance of the QCAC model with respect to

TABLE I
OPTIMALITY GAPS, DISTANCES TO FEASIBILITY, AND RUNTIMES FOR SELECTED PGLIB TEST CASES

	Optimality Gap (%)			Distance to feasibility (p.u.)			Runtime (s)			
Test case	QCAC	SOC	SDP	QCAC	SOC	SDP	QCAC	SOC	SDP	AC
pglib_opf_case30_ieee	0.06256	0.66478	**0.00680**	0.14951	0.29270	**0.00004**	**0.128**	0.105	0.820	0.012
pglib_opf_case39_epri	**0.27498**	3.26863	0.21014	**0.01517**	1.09835	0.07128	**0.028**	0.028	2.820	0.014
pglib_opf_case57_ieee	0.01706	0.00402	**0.00092**	**0.01557**	0.01900	0.01852	0.048	**0.041**	12.387	0.019
pglib_opf_case89_pegase	1.49676	**1.14178**	7.15318	**0.36341**	0.52210	1.18675	**0.754**	0.970	155.698	0.066
pglib_opf_case118_ieee	**0.37494**	2.89311	2.06640	**0.00300**	0.09849	0.06768	**0.141**	0.218	638.261	0.081
pglib_opf_case179_goc	**1.21317**	2.46625	-	**0.02196**	1.32447	-	0.583	**0.192**	-	0.081
pglib_opf_case300_ieee	1.53902	**1.23162**	-	**0.18725**	0.48233	-	3.506	**1.748**	-	0.104
pglib_opf_case500_goc	0.31590	**0.13161**	-	0.01287	**0.01100**	-	**1.687**	2.462	-	0.198
pglib_opf_case793_goc	**0.57544**	3.63319	-	**0.00300**	0.09789	-	**0.781**	1.338	-	0.354
pglib_opf_case1354_pegase	**1.26160**	4.17789	-	**0.01117**	0.53977	-	**2.091**	5.986	-	1.059

The highlighted values correspond to the best out of the QCAC, SOC, and SDP models.

the solution of the original problem. The nonconvex, SOC, and SDP models are solved in PowerModels.jl in JuMP [31]. For each system, we generate 100 demand samples by multiplying the base case's active and reactive power demand by a random vector drawn from a normal distribution with mean 1 and standard deviation 0.1. For all the studied instances, the convexification point for the proposed QCAC approximation is set to be the solution of the base case, which is solved using Knitro.

B. Metrics

1) Optimality gap: We assess the optimality gap of the cost of the projected feasible dispatch of the three models, i.e., QCAC, SOC, and SDP, with respect to the cost of the AC-OPF problem. Such feasible dispatch, which is determined by projecting the approximate dispatches onto the constraint set of the AC-OPF problem, can be obtained by solving the following optimization problem:

$$\bar{\boldsymbol{p}}^{\mathrm{CVX}} \in \arg\min_{\Xi} \quad \|\hat{\boldsymbol{p}}^{\mathrm{CVX}} - \boldsymbol{p}^{g}\|_2^2 \tag{5a}$$
$$\text{subject to} \quad (1\text{b}) - (1\text{n}),$$

where the superscript CVX represents the corresponding convex approximation/relaxations, i.e., $\mathrm{CVX} = \{\mathrm{QCAC}, \mathrm{SOC}, \mathrm{SDP}\}$, and $\bar{\boldsymbol{p}}^{\mathrm{CVX}}$ denotes the Euclidean projection of $\hat{\boldsymbol{p}}^{\mathrm{CVX}}$ onto the constraint set defined by (1b)-(1n). The above optimization problem projects the active power generation dispatch to the feasible set of the AC-OPF problem. Note that Problem (5) is a nonconvex problem and we solve it using Knitro, which is a local solver that produces feasible solutions but not necessarily the closest feasible projection.

The optimality gap is determined as follows:

$$\text{Optimality gap}\,(\%) = 100 \frac{\left| \sum_{k\in\mathcal{G}} C_k\left(\bar{p}_k^{\mathrm{CVX}}\right) - \sum_{k\in\mathcal{G}} C_k\left(p_k^*\right) \right|}{\sum_{k\in\mathcal{G}} C_k\left(p_k^*\right)},$$

where p_k^* denotes the solution of the AC-OPF problem (1).

2) Distance to feasibility: To measure how close the dispatch of the generators of the three models are with respect to the nonconvex constraint set of the AC-OPF problem, we define the distance to feasibility, which corresponds to the root mean square error between $\hat{\boldsymbol{p}}^{\mathrm{g}}$ and its orthogonal projection $\bar{\boldsymbol{p}}^{\mathrm{g}}$, with as follows:

$$\text{Distance to feasibility (p.u.)} = \sqrt{\frac{1}{|\mathcal{G}|}\sum_{k\in\mathcal{G}}\left(\bar{p}_k^{\mathrm{CVX}} - \hat{p}_k^{\mathrm{CVX}}\right)^2}.$$

3) Runtime: For the three models, we report the time to solve the relaxations/approximations in addition to the time to find the closest feasible dispatch, i.e., time to solve Problem (5).

C. Results for small- and medium-scale instances

Table I presents the results for the small to medium-scale instances using the solution of the base case as a convexification point. The SDP relaxation is solved for instances up to 118 buses due to its computational burden. The results show that the proposed approximation is competitive in terms of optimality gap with respect to the other approximate models particularly in the larger instances. In terms of distance to feasibility, the QCAC model notably outperforms the other two models in the majority of test cases, showing its ability to render a more secure generation dispatch. Notice that the quality of the solutions of the proposed approximation might (and often does) depend on how far the operating point is with respect to the convexification point.

D. Results for large-scale instances

We further assess the computational performance in terms of dispatch accuracy and solution speedup of the QCAC model with respect to its nonconvex counterpart using three large-scale test systems of up to 30,000 buses.

Table II summarizes the correlation coefficients and mean/maximum errors of voltage magnitudes, phase angles, and active/reactive power generation. The QCAC model shows high accuracy across the three systems, showing its ability to properly convexify the nonlinearities of the AC-OPF problem. The reactive power is the most challenging variable in terms of both correlation coefficients and absolute errors. Figure 2 illustrates the high correlation of the four variables for an instance of the largest test system.

Figure 3 presents the empirical cumulative distribution functions for all the variables. For the active and reactive

TABLE II
CORRELATION COEFFICIENTS, AND MEAN AND MAXIMUM ERRORS FOR SELECTED PGLIB LARGE-SCALE TEST CASES

Test case	Corr.	Mean error	Max error
Voltage magnitude (p.u.)			
pglib_opf_case6495_rte	0.96352	0.00466	0.22029
pglib_opf_case13659_pegase	0.99348	0.00178	0.15272
pglib_opf_case30000_goc	0.99915	0.00098	0.03687
Phase angle (rad)			
pglib_opf_case6495_rte	0.98937	0.00466	0.31219
pglib_opf_case13659_pegase	0.99697	0.00178	0.31959
pglib_opf_case30000_goc	0.99997	0.00098	0.07397
Active power (p.u.)			
pglib_opf_case6495_rte	0.99227	0.04500	10.40000
pglib_opf_case13659_pegase	0.99831	0.02053	8.28580
pglib_opf_case30000_goc	0.99930	0.00665	1.77600
Reactive power (p.u.)			
pglib_opf_case6495_rte	0.88023	0.06608	7.99996
pglib_opf_case13659_pegase	0.99338	0.01994	3.19172
pglib_opf_case30000_goc	0.97869	0.00601	2.92390

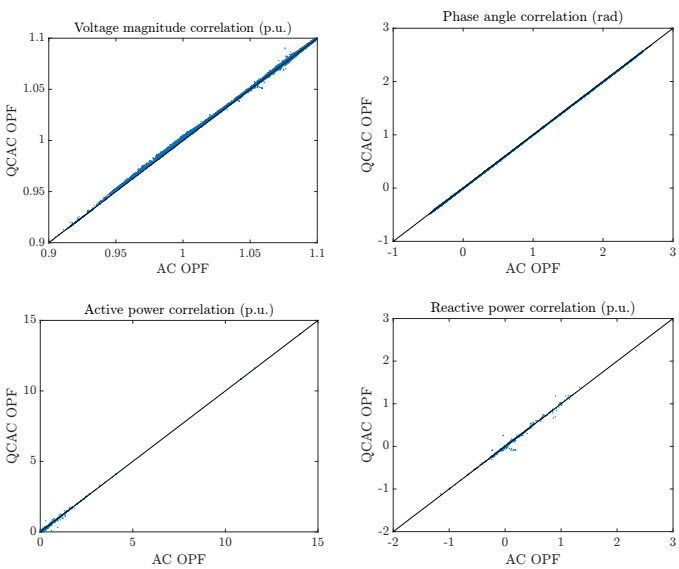

Fig. 2. Correlation of voltage magnitudes, phase angles, and active and reactive power generation for a randomly selected instance of the 30000-bus system

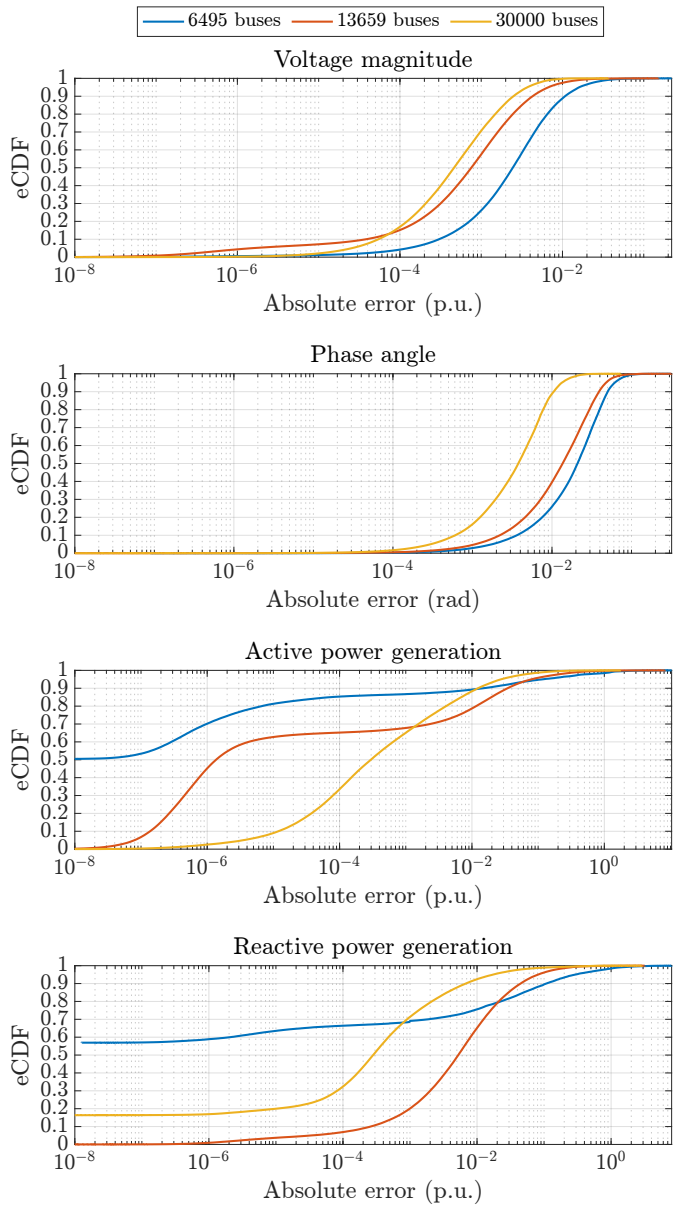

Fig. 3. Empirical cumulative distributions of absolute errors

power generation of the largest system, more than 50% of the instances show an absolute error of less than 1×10^{-8} p.u. The voltage magnitude errors for the three systems are below 0.011 p.u. for 90% of the instances.

Figure 4 shows the time performance profile for the three systems for the QCAC model and the nonconvex AC-OPF problem. The proposed model outperforms the nonconvex model in terms of solution time and reduced runtime variability. The largest system shows the highest runtime speedup, which empirically demonstrates the scalability of the proposed convexified model.

It is important to note that the quality of the solution of the proposed approximation relies heavily on the linearization point as it is the only source of information to convexify the problem. We note that for a standalone application of the QCAC model in real-time operations, a good linearization point can be easily obtained from the last solution of the state estimator. Another alternative to obtain high-quality convexification points is using end-to-end learning-based algorithms, which can predict such points by embedding the QCAC model into the learning pipeline and by leveraging the solution of historical instances.

IV. CASE STUDIES

In this section, we illustrate the application of the proposed approximation in two case studies: optimal reactive power flow with discrete controllers and a PV hosting capacity problem. The case studies indicate that the proposed QCAC model provides an accurate convex approximation of the power flow equations, which is particularly useful when other approximations/relaxations are slow, inaccurate, or neglect

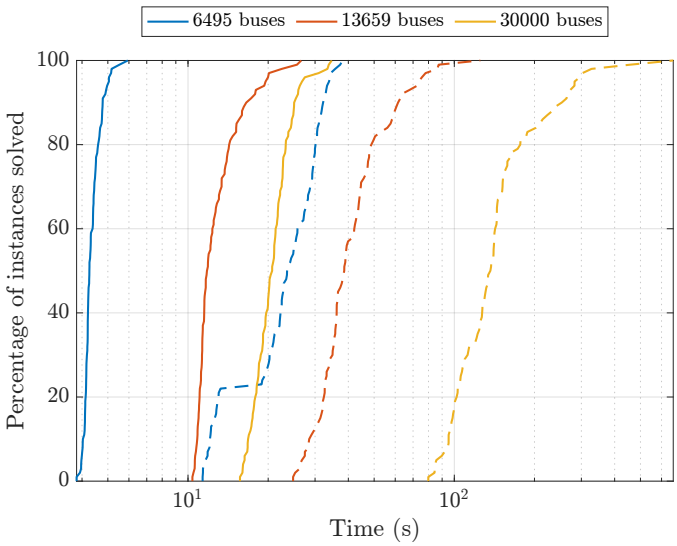

Fig. 4. Time performance profile. QCAC OPF model (Solid). AC OPF model (Dashed).

voltage- and reactive-power-related variables and constraints. The numerical experiments were implemented considering the same setup as in Section IV. Gurobi 11.0.2, Knitro 14.1, and Mosek 10.2.3 as the optimization solvers for the mixed-integer, nonconvex, and convex problems, respectively.

A. Optimal Reactive Power Flow with Discrete Controllers

The optimal reactive power flow (ORPF) problem, a mixed-integer nonconvex problem that derives from the OPF problem, aims at minimizing the generation costs by adjusting the active and reactive power generation setpoints as well as by operating discrete controllers, e.g., switchable shunt reactive power compensation [32], [33]. Operating such discrete controllers aims at acting on the nodal voltages by adjusting the reactive power injections to reduce the generating costs, requiring a detailed representation of both variables, i.e., voltage magnitudes and reactive power flows. Such requirement hinders the use of linear approximations of the power flow equations, such as the DC power flow, that neglect the aforementioned variables.

A simplified formulation of the ORPF problem in lifted rectangular coordinates is presented below:

$$\min_{\Xi} \quad \sum_{k\in\mathcal{G}} C_k(p_k^{\mathrm{g}}) \tag{6a}$$

subject to

$$(1\mathrm{b}), (1\mathrm{d}) - (1\mathrm{n}),$$

$$\sum_{k\in\mathcal{G}_i} q_k^{\mathrm{g}} - Q_i^{\mathrm{d}} + q_i^{\mathrm{sh}} = \sum_{(i,j)\in\mathcal{E}_i} q_{ij} + \sum_{(j,i)\in\mathcal{E}_i} q_{ji}, \ \forall i \in \mathcal{N}, \tag{6b}$$

$$q_i^{\mathrm{sh}} = b_i^{\mathrm{sh}} c_{ii}, \ \forall i \in \mathcal{N}, \tag{6c}$$

$$b_i^{\mathrm{sh}} = \underline{b}_i^{\mathrm{sh}} + \left(\overline{b}_i^{\mathrm{sh}} - \underline{b}_i^{\mathrm{sh}}\right) \frac{n_i^{\mathrm{sh}}}{\overline{n}_i^{\mathrm{sh}}}, \ \forall i \in \mathcal{N}, \tag{6d}$$

$$n_i^{\mathrm{sh}} = \{0, 1, \ldots, \overline{n}_i^{\mathrm{sh}}\}, \ \forall i \in \mathcal{N}, \tag{6e}$$

where the optimization variables are elements of the set:

$$\Xi^{\mathrm{ORPF}} = \{p_k^{\mathrm{g}}, q_k^{\mathrm{g}}, p_{ij}^{\mathrm{fr}}, q_{ij}^{\mathrm{fr}}, p_{ij}^{\mathrm{to}}, q_{ij}^{\mathrm{to}}, q_i^{\mathrm{sh}}, b_i^{\mathrm{sh}}, n_i^{\mathrm{sh}}, c_{ii}, c_{ij}, s_{ij}, v_i^{\mathrm{re}}, v_i^{\mathrm{im}}\}.$$

The objective function (6a) aims at minimizing the total production cost. Constraints (6b) enforce the reactive power balance constraint. Constraints (6c) define the reactive power injected by the shunt compensation per node whereas constraints (6d) define the shunt susceptance per node. Constraints (6e) model the discrete nature of the steps of shunt compensation per node.

The nonconvexities of Problem (6) arise from (i) the bilinear equalities, (6c), (ii) the bilinear and quadratic equalities, (1l)-(1n), and (iii) the discrete variables representing the steps of shunt compensation (6e). The first sources of nonconvexities can be exactly linearized since b_i^{sh} are discrete, and both variables in the bilinear terms are bounded [34, § 9.2]. The interaction of binary variables with the aforementioned nonconvexities makes impractical the solution of the original model for medium or large-scale systems.

To efficiently (approximately) solve Problem (6), we use the QCAC approximation, replacing constraints (1l)-(1n) by (4b)-(4j), rendering in a mixed-integer convex optimization problem, which can be solved by state-of-the-art commercial solvers or well-documented decomposition techniques that exploit convexity, e.g., Benders decomposition. Note as well that the slack variables, $\xi_i^{\mathrm{c}}, \xi_{ij}^{\mathrm{c}}, \xi_{ij}^{\mathrm{s}}$, need to be penalized in the objective function.

To find the convexification point, V_i^{re} and V_i^{im}, we solve the continuous relaxation of Problem (6). The experimental results study the benefits and accuracy of the convexified problem with respect to the original mixed-integer nonconvex formulation and the one using a SOC relaxation of the power flow equations. We use a 30-bus test system [9] under a normal operating condition (TYP) to test the performance of the QCAC approximation.

The solution procedure for using the proposed convex approximation is as follows:

1) Set V_i^{re} and V_i^{im} to the solution of the continuous relaxation of the ORPD problem.
2) Solve the ORPD problem using the convexified constraints (4b)-(4j).
3) Fix n_i^{sh}, b_i^{sh}, and q_i^{sh} to the solution in the previous step, and solve the restricted Problem (6).

In the above procedure, we solve two continuous nonconvex optimization problems to find a convexification point and find a feasible solution for a fixed (near-)optimal value of the discrete controllers, respectively, and a mixed-integer convex problem to find such values for the discrete controllers.

Table III presents the numerical results for the ORPD problem. Gurobi was unable to find a feasible solution to the original MINLP model within 2 hours. Hence, we present the solution of its continuous relaxation, which provides a valid lower bound on the cost. To compute the cost and savings of the QCAC and SOC models, we fix the discrete variables obtained by the corresponding mixed-integer convex approximations and solve the restricted Problem (6), which provides a

TABLE III
RESULTS SUMMARY: PROOF-OF-CONCEPT ORPD PROBLEM

Model	Cost ($)	Savings (%)
AC-OPF	4996.21	-
ORPD†	3974.46	20.45
ORPD with SOC relaxation‡	4272.48	14.49
ORPD with QCAC approximation‡	**4025.62**	**19.43**

† The presented results correspond to the continuous relaxation.
‡ The presented results are obtained following Procedure 1)-3).

feasible solution. Note that the nonconvex problems are solved with Knitro, which cannot guarantee global optimality.

The proposed approximation outperforms the one obtained by using the MISOCP relaxation in terms of cost savings, reducing the production cost by 19.43% compared to the 14.49% of the SOC relaxation. Note as well that techniques such as Benders decomposition, outer approximation, and an active set strategy can be used to reduce the computational burden of solving the problem and enable the scalability [35], [36] of the SOC- and QCAC-based ORPD problems.

B. PV Hosting Capacity Problem

We illustrate the application of the QCAC approximation to a 533-node radial distribution network whose data can be retrieved from Matpower [37]. Particularly, we focus on an application where the SOC relaxation of the power flow equations renders highly inaccurate solutions [38]. One of such applications is the PV hosting capacity problem, which aims to determine the maximum total PV generation that can be accommodated by a distribution feeder without violating its operation limits [39]. The PV hosting capacity problem is formulated as follows:

$$\min_{\Xi^{\text{PVHC}}} \quad -\sum_{i\in\mathcal{N}} p_i^{\text{pv}} \tag{7a}$$

subject to

(1c) – (1n),

$$\sum_{k\in\mathcal{G}_i} p_k^{\text{g}} + p_i^{\text{pv}} - P_i^{\text{d}} - G_i^{\text{sh}} c_{ii} = \sum_{(i,j)\in\mathcal{E}_i} p_{ij} + \sum_{(j,i)\in\mathcal{E}_i} p_{ji}, \quad \forall i \in \mathcal{N}, \tag{7b}$$

$$\overline{P}^{\text{pv}} \geq p_i^{\text{pv}} \geq \underline{P}^{\text{pv}}, \forall i \in \mathcal{N}, \tag{7c}$$

$$p_k^{\text{g}} \geq 0, \forall k \in \mathcal{G}_0, \tag{7d}$$

where the optimization variables are elements of the set:

$$\Xi^{\text{PVHC}} = \{p_k^{\text{g}}, q_k^{\text{g}}, p_i^{\text{pv}}, p_{ij}^{\text{fr}}, q_{ij}^{\text{fr}}, p_{ij}^{\text{to}}, q_{ij}^{\text{to}}, c_{ii}, c_{ij}, s_{ij}, v_i^{\text{re}}, v_i^{\text{im}}\}.$$

The objective function (7a) is to maximize the sum of total power injected by the PV generators connected to a set of predetermined nodes. Constraints (7b) correspond to the nodal balance equations. Constraints (7c) bound the PV power injection per node, whereas constraint (7d) ensures that there is no reverse flow to the substation at the root node, $\mathcal{G}_0$, of the feeder.

The approximated PV hosting problem using the proposed QCAC approximation, can be formulated as follows:

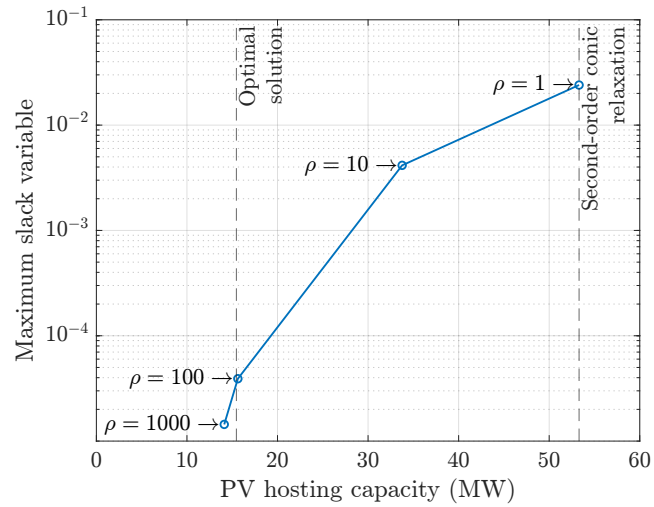

Fig. 5. PV hosting capacity: Maximum slack-variable penalty trade-off curve.

$$\min_{\Xi^{\text{PVHC}}} \quad -\sum_{i\in\mathcal{N}} p_i^{\text{pv}} + \rho\left[\sum_{i\in\mathcal{N}} \xi_i^{\text{c}} + \sum_{(i,j)\in\mathcal{E}} \left(\xi_{ij}^{\text{c}} + \xi_{ij}^{\text{s}}\right)\right] \tag{8a}$$

subject to

(1c) – (1k), (4b) – (4j), (7b) – (7d),

where the optimization variables are elements of the set:

$$\Xi^{\text{PVHC}} = \{p_k^{\text{g}}, q_k^{\text{g}}, p_i^{\text{pv}}, p_{ij}^{\text{fr}}, q_{ij}^{\text{fr}}, p_{ij}^{\text{to}}, q_{ij}^{\text{to}}, c_{ii}, c_{ij}, s_{ij}, v_i^{\text{re}}, v_i^{\text{im}}, \xi_i^{\text{c}}, \xi_{ij}^{\text{c}}, \xi_{ij}^{\text{s}}\}.$$

The convexification points of the power flow equations are set to a flat voltage profile. Figure (5) illustrates a frontier of the maximum slack variable and the PV hosting capacity for different values of the penalty coefficient ρ. Note that higher values of the penalty coefficient result in more conservative solutions that are closer to being feasible and to the convexification point. For $\rho = 100$, the approximated problem results in a near-optimal and near-feasible solution with a maximum slack variable of 4×10^{-5}. For $\rho = 1$, the approximated problem results in the same optimal objective function value as using the SOC relaxation with a maximum slack variable of 2.5×10^{-2}, which is highly infeasible. Note as well that according to the optimal value of the objective function, the SOC relaxation for this problem is a loose relaxation of the power flow equations.

Table IV summarizes the results of the three models, i.e., nonconvex, SOC, and QCAC. For all the penalty coefficients, the proposed model offers a speedup of $\approx 33\times$ on average with the best cost error of $\approx 1\%$ whereas the SOC relaxation shows a higher speed up of $45\times$, but with a significantly higher cost error of $\approx 245\%$.

V. CONCLUSION

In this paper, we propose a quadratically-constrained convex approximation for the AC-OPF problem that relies solely on a convexification point, without the need for additional assumptions. The approach is based on a difference-of-convex

TABLE IV
RESULT SUMMARY: PV HOSTING CAPACITY PROBLEM

Model	ρ	Cost (MW)	Cost error (%)	Speedup
Nonconvex	-	15.458	-	-
SOC relaxation	-	53.300	244.80	44.8
QCAC approximation	1	53.300	244.80	41.4
	10	33.763	118.42	33.6
	100	**15.623**	**1.07**	29.5
	1000	14.118	8.67	27.5

reformulation of the power flow equations, followed by a convexification procedure using a first-order Taylor series expansion of the resulting concave terms. Our extensive numerical results demonstrate the advantages of this model, including a reduced optimality gap, near-feasible solutions, and smaller solution errors compared to the nonconvex AC formulation. Furthermore, two proof-of-concept case studies illustrate the potential benefits of the proposed approximation over the second-order conic and semidefinite relaxations of the power flow equations.

In our future work, we plan to make the proposed approximation adaptive in the sense that the convexification point and penalty coefficient are tuned to minimize the approximation error for a given operating range. We additionally plan to apply the proposed model to other applications such as a AC security-constrained unit commitment problem, transmission expansion planning problems, distribution OPF problem with distributed generation, and the robust OPF problem.

REFERENCES

[1] F. Capitanescu, "Critical review of recent advances and further developments needed in AC optimal power flow," *Electric Power Systems Research*, vol. 136, pp. 57–68, 7 2016.

[2] X. Bai, H. Wei, K. Fujisawa, and Y. Wang, "Semidefinite programming for optimal power flow problems," *International Journal of Electrical Power & Energy Systems*, vol. 30, pp. 383–392, 7 2008.

[3] R. A. Jabr, "Radial distribution load flow using conic programming," *IEEE Transactions on Power Systems*, vol. 21, pp. 1458–1459, 8 2006.

[4] C. Coffrin, H. L. Hijazi, and P. V. Hentenryck, "The QC relaxation: A theoretical and computational study on optimal power flow," *IEEE Transactions on Power Systems*, vol. 31, pp. 3008–3018, 7 2016.

[5] C. Chen, A. Atamturk, and S. S. Oren, "Bound tightening for the alternating current optimal power flow problem," *IEEE Transactions on Power Systems*, vol. 31, pp. 3729–3736, 9 2016.

[6] S. Sojoudi and J. Lavaei, "Physics of power networks makes hard optimization problems easy to solve," in *2012 IEEE Power and Energy Society General Meeting*, 2012, pp. 1–8.

[7] D. K. Molzahn and I. A. Hiskens, "A survey of relaxations and approximations of the power flow equations," *Foundations and Trends® in Electric Energy Systems*, vol. 4, pp. 1–221, 2019.

[8] C. Coffrin and P. V. Hentenryck, "A linear-programming approximation of AC power flows," *INFORMS Journal on Computing*, vol. 26, pp. 718–734, 5 2014, doi: 10.1287/ijoc.2014.0594.

[9] O. Alsac and B. Stott, "Optimal load flow with steady-state security," *IEEE Transactions on Power Apparatus and Systems*, vol. PAS-93, no. 3, pp. 745–751, 1974.

[10] A. Castillo, P. Lipka, J. P. Watson, S. S. Oren, and R. P. O'Neill, "A successive linear programming approach to solving the IV-ACOPF," *IEEE Transactions on Power Systems*, vol. 31, pp. 2752–2763, 2016.

[11] S. Pineda, J. Pérez-Ruiz, and J. M. Morales, "Beyond the neural fog: Interpretable learning for AC optimal power flow," 2024. [Online]. Available: https://arxiv.org/abs/2408.05228

[12] H. Zhang, G. T. Heydt, V. Vittal, and J. Quintero, "An improved network model for transmission expansion planning considering reactive power and network losses," *IEEE Transactions on Power Systems*, vol. 28, no. 3, pp. 3471–3479, 2013.

[13] Z. Yang, H. Zhong, Q. Xia, and C. Kang, "A novel network model for optimal power flow with reactive power and network losses," *Electric Power Systems Research*, vol. 144, pp. 63–71, 3 2017.

[14] Z. Yang, H. Zhong, A. Bose, T. Zheng, Q. Xia, and C. Kang, "A linearized OPF model with reactive power and voltage magnitude: A pathway to improve the MW-only DC OPF," *IEEE Transactions on Power Systems*, vol. 33, no. 2, pp. 1734–1745, 2018.

[15] S. M. Fatemi, S. Abedi, G. B. Gharehpetian, S. H. Hosseinian, and M. Abedi, "Introducing a novel DC power flow method with reactive power considerations," *IEEE Transactions on Power Systems*, vol. 30, no. 6, pp. 3012–3023, 2015.

[16] Z. Li, J. Yu, and Q. H. Wu, "Approximate linear power flow using logarithmic transform of voltage magnitudes with reactive power and transmission loss consideration," *IEEE Transactions on Power Systems*, vol. 33, no. 4, pp. 4593–4603, 2018.

[17] Z. Yang, K. Xie, J. Yu, H. Zhong, N. Zhang, and Q. Xia, "A general formulation of linear power flow models: Basic theory and error analysis," *IEEE Transactions on Power Systems*, vol. 34, no. 2, pp. 1315–1324, 2019.

[18] Z. Fan, Z. Yang, J. Yu, K. Xie, and G. Yang, "Minimize linearization error of power flow model based on optimal selection of variable space," *IEEE Transactions on Power Systems*, vol. 36, no. 2, pp. 1130–1140, 2021.

[19] J. Long, Z. Yang, J. Zhao, and J. Yu, "Modular linear power flow model against large fluctuations," *IEEE Transactions on Power Systems*, vol. 39, no. 1, pp. 402–415, 2024.

[20] R. P. O'Neill, A. Castillo, and M. B. Cain, "The IV formulation and linear approximations of the AC optimal power flow problem," *Federal Energy Regulatory Commission*, 2012.

[21] S. Mhanna and P. Mancarella, "An exact sequential linear programming algorithm for the optimal power flow problem," *IEEE Transactions on Power Systems*, vol. 37, no. 1, pp. 666–679, 2022.

[22] S. Bolognani and F. Dörfler, "Fast power system analysis via implicit linearization of the power flow manifold," in *2015 53rd Annual Allerton Conference on Communication, Control, and Computing (Allerton)*, 2015, pp. 402–409.

[23] C. Coffrin, H. Hijazi, and P. V. Hentenryck, "Alternating current (AC) power flow analysis in an electrical power network," 2012, U.S. Patent 20150088439.

[24] M. Baradar and M. R. Hesamzadeh, "AC power flow representation in conic format," *IEEE Transactions on Power Systems*, vol. 30, no. 1, pp. 546–547, 2015.

[25] K. Šepetanc and H. Pandžić, "Convex polar second-order Taylor approximation of AC power flows: A unit commitment study," *IEEE Transactions on Power Systems*, vol. 36, no. 4, pp. 3585–3594, 2021.

[26] S. Merkli, A. Domahidi, J. L. Jerez, M. Morari, and R. S. Smith, "Fast AC power flow optimization using difference of convex functions programming," *IEEE Transactions on Power Systems*, vol. 33, no. 1, pp. 363–372, 2018.

[27] T. Lipp and S. Boyd, "Variations and extension of the convex–concave procedure," *Optimization and Engineering*, vol. 17, pp. 263–287, 2016.

[28] M. Besançon, J. Dias Garcia, B. Legat, and A. Sharma, "Flexible differentiable optimization via model transformations," *INFORMS Journal on Computing*.

[29] A. Agrawal, B. Amos, S. Barratt, S. Boyd, S. Diamond, and Z. Kolter, "Differentiable convex optimization layers," in *Advances in Neural Information Processing Systems*, 2019.

[30] S. Babaeinejadsarookolaee, A. Birchfield, R. D. Christie, C. Coffrin, C. DeMarco, R. Diao, M. Ferris, S. Fliscounakis, S. Greene, R. Huang, C. Josz, R. Korab, B. Lesieutre, J. Maeght, T. W. K. Mak, D. K. Molzahn, T. J. Overbye, P. Panciatici, B. Park, J. Snodgrass, A. Tbaileh, P. V. Hentenryck, and R. Zimmerman, "The Power Grid Library for benchmarking AC optimal power flow algorithms," 2021.

[31] C. Coffrin, R. Bent, K. Sundar, Y. Ng, and M. Lubin, "Powermodels.jl: An open-source framework for exploring power flow formulations," in *2018 Power Systems Computation Conference (PSCC)*, June 2018, pp. 1–8.

[32] Z. Yang, A. Bose, H. Zhong, N. Zhang, Q. Xia, and C. Kang, "Optimal reactive power dispatch with accurately modeled discrete control devices: A successive linear approximation approach," *IEEE Transactions on Power Systems*, vol. 32, no. 3, pp. 2435–2444, 2017.

[33] S. G. Constante F., J. C. López, and M. J. Rider, "Optimal reactive power dispatch with discrete controllers using a branch-and-bound algorithm: A

semidefinite relaxation approach," *IEEE Transactions on Power Systems*, vol. 36, no. 5, pp. 4539–4550, 2021.

[34] H. Williams, *Model Building in Mathematical Programming*, 5th ed. Wiley, 2013.

[35] G. E. Constante-Flores, A. J. Conejo, and F. Qiu, "Daily scheduling of generating units with natural-gas market constraints," *European Journal of Operational Research*, vol. 313, pp. 387–399, 2024.

[36] R. A. Jabr, "Outer approximation method for discrete AC optimal power flow," *IEEE Transactions on Power Systems*, pp. 1–12, 2024.

[37] R. D. Zimmerman, C. E. Murillo-Sanchez, and R. J. Thomas, "Matpower: Steady-state operations, planning, and analysis tools for power systems research and education," *IEEE Transactions on Power Systems*, vol. 26, pp. 12–19, 2 2011.

[38] S. H. Low, "Convex relaxation of optimal power flow—Part II: Exactness," *IEEE Transactions on Control of Network Systems*, vol. 1, no. 2, pp. 177–189, 2014.

[39] R. R. Jha, A. Inaolaji, B. D. Biswas, A. Suresh, A. Dubey, S. Paudyal, and S. Kamalasadan, "Distribution grid optimal power flow (D-OPF): Modeling, analysis, and benchmarking," *IEEE Transactions on Power Systems*, vol. 38, no. 4, pp. 3654–3668, 2023.